

Total-capture cross sections for very slow Ar^{4+} -Ar and Ar^{6+} -Ar collisions

C. Biedermann, J.C. Levin, R.T. Short, S.B. Elston, J.P. Gibbons, and I.A. Sellin
Department of Physics, University of Tennessee, Knoxville, Tennessee 37996-1200
and Oak Ridge National Laboratory, Oak Ridge, Tennessee 37831-6377

H. Cederquist, L.R. Andersson, H. Andersson, and L. Liljeby
Manne Siegbahn Institute of Physics, S-10405 Stockholm, Sweden

(Received 19 July 1990)

We present experimental and calculated total single-electron capture cross sections for Ar^{4+} -Ar collisions in the laboratory energy ranges 100–800 and 10–800 eV, respectively. The experimental results for post-collisional energy and angular distributions of Ar^{3+} extend down to 19 eV; below 100 eV a part of the angular distribution falls outside the $\pm 9^\circ$ angular acceptance. The absolute calibration of our Ar^{4+} -Ar results is achieved by means of normalization of relative Ar^{6+} -Ar single-capture cross sections to absolute total cross sections from the literature. Calculated single-electron capture cross sections for Ar^{4+} -Ar are obtained from a multichannel Landau-Zener model with semiempirical coupling strengths that reproduce the experimental state-selective angular distributions. When these theoretical angular distributions are integrated over the experimental angular acceptance, the agreement between experimental and calculated cross sections is excellent down to 19 eV. We also present total experimental cross sections for removing two electrons from Ar for collisions with Ar^{6+} at 800, 600, and 450 eV, and for 800 eV collisions with Ar^{4+} .

I. INTRODUCTION

We reported in an earlier paper¹ on the comparison between experimental and calculated state-selective angular distributions for one- and two-electron processes in very slow Ar^{4+} -Ar collisions. The earlier experimental results ranged down to a laboratory energy of 19 eV for single-electron capture and down to 150 eV for true double capture and transfer ionization. A seven-channel classical trajectory Landau-Zener calculation reproduced the experimental angular distributions for single-electron capture over a wide energy range (19–800 eV) when the angular-momentum properties of the separated initial and final atomic states were taken into account in the semi-empirical coupling strengths.¹ In this Brief Report we present calculations of the corresponding total cross sections for single-electron capture and compare with our new experimental results for absolute total cross-sections. We have established an absolute experimental cross-section scale through measurements of state-selective angular differential capture cross sections for Ar^{6+} on Ar, which we normalize to absolute total single-capture cross sections from Nielsen *et al.*²

II. EXPERIMENTAL METHOD

The experimental setup has been described in detail elsewhere^{1,3} and therefore we only give a brief summary here. Very slow recoil ions are produced by means of a tightly collimated fast heavy-ion beam, which impinges on a differentially pumped Ar-gas target. The Ar ions are

extracted by an electric field, which is kept small in order to limit the energy spread of the extracted beam. The recoil ion beam is accelerated to a Wien filter for charge-state selection and then retarded and collimated before it interacts with an effusive gas-jet target. Charge states, energies, and scattering angles of the emerging projectiles are determined with the aid of a cylindrical electrostatic analyzer and a two-dimensional position-sensitive detector. The angular acceptance of the detector system is $\pm 9^\circ$. The target gas pressure has been varied in order to assure single-collision conditions. We have assumed that the detection efficiency of the apparatus is the same for the primary and for the charge-exchanged components of the beam, since the operating voltage of the position-sensitive detector was well inside the region of constant detection efficiency. The use of a gas-jet target for the slow collisions makes it impossible to determine the target thickness directly. Instead, we have calibrated this quantity by comparisons of Ar^{6+} -Ar cross sections with results published by Nielsen *et al.*²

III. RESULTS AND DISCUSSION

The angular differential cross sections $d\sigma/d\Omega$ for single-electron capture (solid line) and double-electron capture (dashed line) for Ar^{6+} -Ar collisions are shown in Fig. 1 at the collision energies (a) 100, (b) 300, (c) 450, (d) 600, and (e) 800 eV. The intensity for single-electron capture is plotted at one-tenth of its value for reasons of clarity. The horizontal bars indicate the full width at half maximum for the incident Ar^{6+} beam profile. Nielsen

*et al.*² report on an angular acceptance of $\pm 5^\circ$ and an overall uncertainty in the absolute cross-section scale of 30%. As can be seen from Fig. 1, the angular distributions fall within the $\pm 5^\circ$ limits at energies down to 450 eV. We thus use the results of Nielsen *et al.*² at 500 and 1000 eV and assume that the total single-capture cross section increases linearly between 4.8×10^{-15} cm²

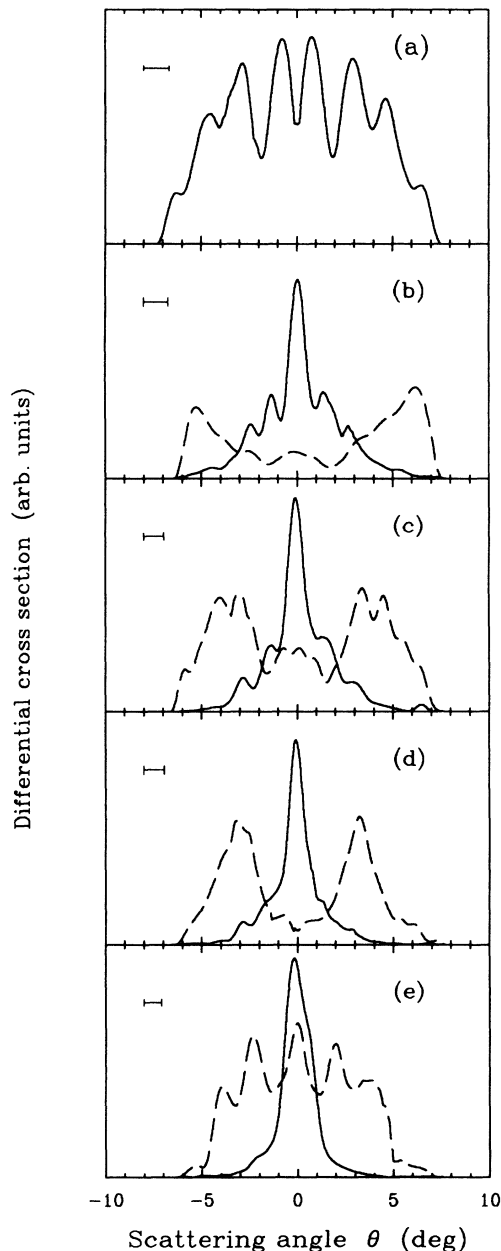


FIG. 1. Experimental angular differential cross sections $d\sigma(\theta)/d\Omega$ for single-electron capture (solid line) and double-electron capture (dashed line) in Ar^{6+} -Ar collisions at laboratory energies of (a) 100, (b) 300, (c) 450, (d) 600, and (e) 800 eV. The single-capture intensity is shown at one-tenth of its true value in order to fit the scale. The horizontal bars indicate the full width at half maximum (FWHM) of the incident Ar^{6+} -beam profile.

and 5.3×10^{-15} cm² when the energy increases from 500 to 1000 eV. Our total cross sections for 600 and 800 eV fall on the straight line between the 500- and 1000-eV data points from Nielsen *et al.*² when the ratios between our Ar^{5+} and Ar^{6+} rates are divided by a common target thickness. In this way we determine the target thickness for a specific setting of the driving pressure for the gas jet, which we then use in the Ar^{4+} -Ar experiment to set the absolute cross-section scale to an accuracy of 30%.² The present result at 100 eV exceeds the one by Nielsen *et al.*² by roughly 50%. The reason is seen in Fig. 1, which shows that at 100 eV the angular distribution extends considerably outside the $\pm 5^\circ$ range. The angular distributions for single-electron capture and true double-electron capture shown in Fig. 1 indicate that the present (open circles) total cross sections for single capture (SC) and double capture (DC) plotted in Fig. 2 are reliable down to roughly 300 and 450 eV, respectively. At lower energies, scattering outside the $\pm 9^\circ$ experimental acceptance occurs. The problem of losing projectiles due to large scattering angles has been addressed by, e.g., Olson and Kimura,⁴ who estimated large angle scattering in low-energy ion-atom collisions. With the measurement of angular distributions as a function of the collision energy we can monitor the intensity loss due to large scattering angles closely. Total cross sections from the extended classical over barrier model⁵ (ECB) are indicated with arrows in Fig. 2.

Experimental total Ar^{4+} -Ar cross sections for single-electron capture (circles) and the sum of true double-electron capture and transfer ionization cross sections at 800 eV (triangle) are shown in Fig. 3. In the true double-capture process two electrons are transferred between the target and a nonautoionizing projectile state, whereas the transfer ionization process involves emission

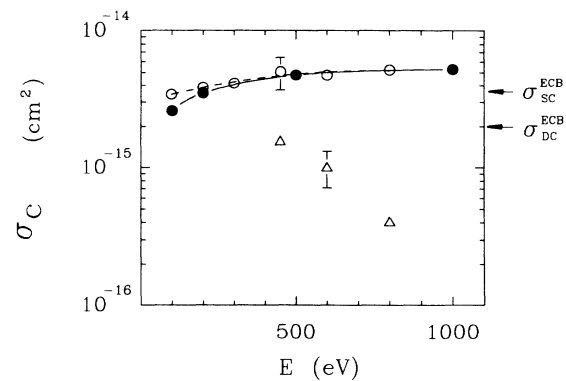


FIG. 2. Total experimental cross sections for single-electron capture (circles) and the sum of the cross sections for double-electron capture and transfer ionization (triangles) in Ar^{6+} -Ar collisions. The present results of single capture (open circles) are normalized to the data from Ref. 2 (solid circles) in the collision energy range above 500 eV. The uncertainty in the absolute scale is 30%. The magnitudes of the cross sections from the extended classical over barrier model (ECB) for removing one (SC) and two (DC) electrons from the target are indicated by arrows. Lines are to guide the eye.

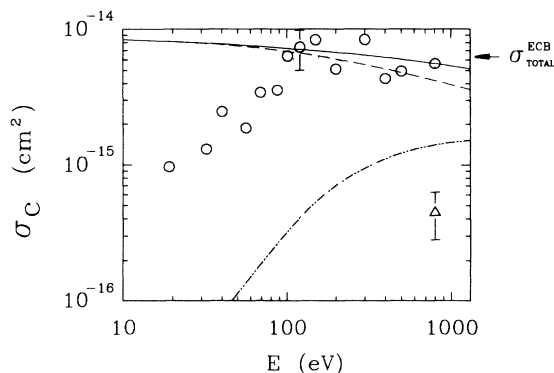


FIG. 3. Total experimental and calculated electron-capture cross sections for Ar^{4+} -Ar collisions. Total experimental single-capture cross sections (circles) are compared with the corresponding total model cross sections (solid line). The dashed and the dash-double-dotted lines are the calculated cross sections for capture to the Ar^{3+} $4p$ and the Ar^{3+} $4s$ levels, respectively. The dotted line represents calculated single-capture cross sections within the experimental acceptance angle of $\pm 9^\circ$. The sum of the experimental cross sections for double-electron capture and transfer ionization at 800 eV is shown by a triangle. The uncertainty in the absolute scale is 30% for experimental cross sections. The total ECB cross section for electron removal is indicated with an arrow (cf. text).

of one electron after the collision. The models we discuss here cannot differentiate between transfer ionization and true double capture. Therefore we have added the contributions from these two cross sections. Total and partial cross sections from a seven-channel classical-trajectory Landau-Zener model¹ used to interpret the structures in the angular distributions are shown in the same figure, while ECB cross sections are indicated by arrows. The solid line in Fig. 3 represents the total single-capture cross section, which is taken to be the sum of the cross sections for capture to the $4p$ (dashed line) and the $4s$ (dash-double-dotted line) levels. The $4p$ cross section is in turn the sum of the contributions from six unresolved $4p$ LS terms. The total model cross section for a given channel i is taken as

$$\sigma_i = 2\pi \int_0^\infty P_i(b) b db,$$

where $P_i(b)$ is the transition probability for populating channel i . For $P_i(b)$ we use the multichannel Landau-Zener expression (see, e.g., Ref. 6), while the coupling matrix elements are given in Ref. 1. In order to make a quantitative comparison between measured and calculated cross sections at the lower energies, we take into account that the experiment discriminates against scattering angles larger than 9° . The dotted line in Fig. 3 represents the partial single-electron capture cross section obtained by integration of the calculated differential cross sections (Ref. 1) over the angular interval 0 to 9° ,

$$\hat{\sigma}_i = 2\pi \int_{0^\circ}^{9^\circ} \sin \theta \frac{d\sigma_i(\theta)}{d\Omega} d\theta,$$

and summation over all (seven) open single-capture channels. The resulting calculated partial cross sections are consistent with the ones measured within the $\pm 9^\circ$ angular range. It is evident from measured energy-gain spectra¹ that the population of $4p$ terms dominates by more than one order of magnitude for collision energies below about 200 eV. At higher collision energies the contribution of single capture to the $4s$ level increases.⁷⁻⁹ We argue in detail in our recent paper¹ on state-selective angular distributions for Ar^{4+} -Ar collisions that metastable Ar^{4+} does not affect the energy-gain spectra or the angular distributions. We have considered capture to the six unresolved $4p$ and to the outermost of two $4s$ levels in the calculation, while we assume that the innermost $4s$ level couples fully adiabatically to the incident channel. We believe that this is sufficient to describe the total single-electron capture cross section since both our experiment and calculation show that the outermost $4s$ channel is weakly populated at 800 eV and that the outermost $4p$ terms (crossings near ~ 12 a.u.) still are of diabatic character at the lowest energy of 19 eV. Thus it is reasonable to neglect contributions from the $4d$ levels of Ar^{3+} which cross the incident channel at ~ 25 a.u. The slight increase in the total model single-capture cross section with decreasing energy which we observe here is expected for a system with sufficiently high densities of capture levels in the region of internuclear distances where electron transfer is effective. That is, distant crossings become less diabatic as the collision velocity is lowered. This rather weak velocity dependence is not reproduced by the static ECB model.⁵ It is, however, worthwhile to note that the ECB model gives a reasonable prediction of the total single-capture cross section, as expected for a system with a high density of final capture states. (In Fig. 3 we compare the experimental total single-capture cross section with the total ECB cross section for electron removal since the experimental double-capture cross section is found to be very small.) In Fig. 3 we also show the sum of the experimental total cross sections (triangle) for true double-electron capture and transfer ionization for Ar^{4+} -Ar collisions at 800 eV. At lower energies parts of the angular distributions for two-electron processes fall outside the experimental acceptance and no total cross sections can be deduced.¹ We have concluded before¹ that double-electron capture predominantly takes place via a two-step process. This conclusion has also been reached by Koslowski and Huber,⁸ who estimated a total double-capture cross section in good agreement with the present experimental value at 800 eV.

Earlier we showed¹ that inclusion of the angular momentum properties of the separated projectile and target in the evaluations of adiabatic coupling strengths is essential in order to reproduce the experimental state-selective angular distributions. Here we see that the same method gives good agreement for the total single-capture cross section over a large velocity range. The good agreement between the measured and calculated cross sections within the experimental angular acceptance strongly sup-

TABLE I. Total experimental cross sections for one- and two-electron capture in Ar^{4+} -Ar and Ar^{6+} -Ar collisions. Cross sections are given in units of 10^{-16} cm^2 . For Ar^{6+} -Ar collisions we compare to the data of Nielsen *et al.* (Ref. 2). The overall uncertainty in the absolute scale is 30%.

E (eV)	Ar^{4+} -Ar		Ar^{6+} -Ar		
	Single capture	Double capture	Single capture		Double capture
			Present data	Ref. 2	Present data
1000				53	
800	56	5	52		4
600			48		10
500	50			48	
450			51		16
400	44				
300	84		42		
200	51				
150	84				
100	64				

ports the use of the multichannel Landau-Zener model for calculating single-electron capture cross sections at the present level of accuracy. We have illustrated that the recording of angular distributions is essential in order to avoid underestimation of total cross sections due to large-angle scattering. Total capture cross sections for processes that have been found to be detectable within the experimental angular acceptance are presented in Table I.

ACKNOWLEDGMENTS

This work was supported in part by the National Science Foundation; by the U.S. Department of Energy, Office of Basic Energy Sciences, Division of Chemical Sciences, under Contract No. DE-AC05-84OR21400 with Martin Marietta Energy Systems Inc.; and by the Swedish Natural Science Research Council.

¹C. Biedermann, H. Cederquist, L.R. Andersson, J.C. Levin, R.T. Short, S.B. Elston, J.P. Gibbons, H. Andersson, L. Liljeby, and I.A. Sellin, *Phys. Rev. A* **41**, 5889 (1990).

²E.H. Nielsen, L.H. Andersen, A. Bárány, H. Cederquist, P. Hvelplund, H. Knudsen, K.B. MacAdam, and J. Sørensen, *J. Phys. B* **17**, L139 (1984).

³H. Cederquist, C. Biedermann, J.C. Levin, C.-S. O, I.A. Sellin, and R.T. Short, *Nucl. Instrum. Methods B* **34**, 243 (1988).

⁴R.E. Olson and M. Kimura, *J. Phys. B* **15**, 4231 (1982).

⁵A. Bárány, G. Astner, H. Cederquist, H. Danared, S. Huldt, P. Hvelplund, A. Johnson, H. Knudsen, L. Liljeby, and K.-G. Rensfelt, *Nucl. Instrum. Methods B* **9**, 397 (1985).

⁶A. Salop and R.E. Olson, *Phys. Rev. A* **13**, 1312 (1976).

⁷J.P. Giese, C.L. Cocke, W. Waggoner, L.N. Tunnell, and S.L. Varghese, *Phys. Rev. A* **34**, 3770 (1986).

⁸H.R. Koslowski and B.A. Huber, *J. Phys. B* **22**, 2255 (1989).

⁹J. Puerta, H.-J. Kahlert, H.R. Koslowski, and B.A. Huber, *Nucl. Instrum. Methods B* **9**, 415 (1985).